Journal of Russian Laser Research, Volume 21, Number 6, 2000

COMBINED DIFFRACTION GRATING IN THE SCHEME OF GRAZING INCIDENCE: CALCULATION AND PARAMETER OPTIMIZATION

S. V. Vasil'ev, V. A. Sychugov, and B. A. Usievich

Institute of General Physics, Russian Academy of Sciences, Ul. Vavilova, 38, Moscow 117942, Russia
e-mail: borisu@kapella.gpi.ru

Abstract

The method of parameter optimization of combined structures, which consist of a dielectric grating and a metallic or multilayer dielectric mirror, was proposed. It is based on the use of the waveguide properties of the combined diffraction grating. Its main advantage lies in the possibility of determining the optimum parameters of the combined grating without solving the diffraction problem.

1. Introduction

With the development of lasers the requirements for the elemental basis of laser devices and, in particular, for the radiation stability and efficiency of the diffraction gratings became more stringent. The use of conventional metallic gratings is hampered or becomes impossible in solving a number of problems associated with the development of pulsed narrow-band and superradiant lasers.

The creation of combined gratings, which was proposed in [1] for the first time, was a decisive step toward improving the characteristics of diffraction gratings. In Fig. 1, the schematic diagram of a combined diffraction grating is presented. The grating by itself is formed in the dielectric layer G. There is an interlayer S under the grating followed by a metallic or multilayer dielectric mirror M. Such gratings possess a number of significant properties from the practical point of view. Combined diffraction gratings with an extremely high diffraction efficiency and radiation stability designated for pulse compression were described in [2, 3]. Studies of the properties of combined gratings set in the scheme of grazing incidence were the focus of [4, 5]. As was shown in these papers, the efficiency of the combined grating with a metallic mirror could far exceed that of the conventional grating with a metal coating at a comparable absorption level.

Given the wavelength and angle of incidence of radiation as well as the material refractive indices and grating profile, the problem of determination of the parameters of the most efficient grating is reduced to the search for the optimum values of the grating depth $h^{(G)}$, interlayer thickness $h^{(S)}$, and (in the case of the grating with a dielectric mirror) thickness of the layers of the mirror $h_i^{(M)}$. A rigorous solution of the problem of diffraction by a combined grating requires a significant volume of calculations. The time taken to calculate the diffraction efficiencies of the grating with preassigned parameters with a contemporary PC varies from several seconds to several tens of seconds. The authors' experience in studying combined gratings suggests that the dependence of the diffraction efficiency of such a grating on the layer thickness has a lot of extremums. These factors render the use of the techniques of numerical optimization of parameters for the multilayered combined grating to be extremely inefficient.

In the present paper, a procedure is proposed that allows one to determine the optimum parameters of the combined grating in an analytical form or using much smaller computational resources as compared to the case of direct optimization. An approach based on the waveguide properties of the combined grating was employed

Translated from a manuscript submitted August 30, 2000.

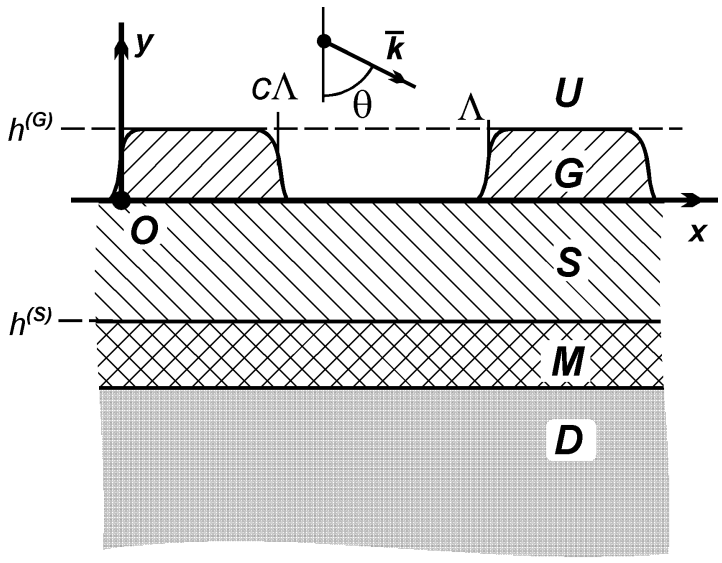

Fig. 1. Schematic diagram of the combined diffraction grating. Here, U is the upper half-space; G, the layer of the diffraction grating; S, the matching dielectric layer; M, the metallic or dielectric mirror; D, the lower half-space; k, the wave vector of the incident wave; θ, the angle of incidence of radiation; Λ, the grating period; and c, the filling factor of the grating.

for the solution of this problem. The waveguide behavior of the interaction of light with the combined grating was demonstrated in [1]. This allowed an analytical expression to be obtained for the efficiency of the metal–dielectric combined grating with a small corrugation depth operating in the autocollimation mode. In this paper, the waveguide approach was extended to more complex structures and arbitrary conditions of radiation incidence.

2. Interaction of Radiation with the Combined Diffraction Grating

A so-called modal technique of solution of the problem of diffraction by the grating was used in the calculations. A detailed description of it can be found in [6]. We focus on the basic specific features of this method, which will help us to interpret the results obtained.

Let a plane electromagnetic wave be incident on the grating G from the upper half-space U. The field distribution resulting from the diffraction of radiation by the grating should satisfy the Helmholtz equation

$$\left(\frac{\partial^2}{\partial x^2} + \frac{\partial^2}{\partial y^2} + k^2(x,y)\right) F(x,y) = 0, \tag{1}$$

the quasiperiodicity condition

$$\exp(ikn^{(U)} \sin\theta\Lambda) F(x,y) = F(x+\Lambda, y), \tag{2}$$

and continuity conditions at the boundaries of the spatial regions with different refractive indices. The function $F(x,y)$ describes either the E or H field component depending on the polarization, $k = 2\pi/\lambda$ is the wave vector of the incident wave, θ is the angle of incidence of radiation upon the grating, and Λ is the grating period.

The solution of problem (1), (2) in the upper (U) and lower (D) half-spaces is the so-called Rayleigh expansion

$$F^{(U)}(x,y) = r^{(i)} \exp(i\alpha_0 x - i\beta_0^{(U)} y) + \sum_{n=-\infty}^{n=+\infty} r_n \exp(i\alpha_n x + i\beta_n^{(U)} y),$$
$$F^{(D)}(x,y) = \sum_{n=-\infty}^{n=+\infty} t_n \exp(i\alpha_n x - i\beta_n^{(D)} y), \tag{3}$$

where $\alpha_n = kn^{(U)} \sin\theta + (2\pi/\Lambda)n$ and $\beta_n^{(j)2} = k^2 n^{(j)2} - \alpha_n^2$. The radiation diffraction orders, which carry away energy from the grating, correspond to the terms of expansion with real coefficients $\beta_n^{(j)}$. The number of such diffraction orders is defined by the relationship between the radiation wavelength and the grating period and, when the diffraction to the lower half-space is concerned, by the refractive index $n^{(D)}$ of the grating substrate.

The solution of problem (1), (2) in the interlayer S and layers of mirror M is also the Rayleigh expansion

$$F^{(S,M)}(x,y) = \sum_m \left[a_m^{(S,M)} \exp(i\beta_m^{(S,M)} y) + b_m^{(S,M)} \exp(-i\beta_m^{(S,M)} y) \right] \exp(i\alpha_m x), \tag{4}$$

but in contrast to expansions (3) they simultaneously contain terms corresponding to the waves, which travel both in the positive and negative direction of the Oy axis.

For a rectangular ruling one can separate the variables in Eq. (1) and construct an analytical expression for the field in the vicinity of grating G:

$$F^{(G)}(x,y) = \sum_m \left[a_m^{(G)} \exp(i\mu_m y) + b_m^{(G)} \exp(-i\mu_m y) \right] u_m(x). \tag{5}$$

The constants μ_m and the form of functions $u_m(x)$ in mode expansion (5) are determined when solving the eigenvalue problem. The latter arises when integrating Eq. (1) with allowance made for the quasiperiodicity condition (2) and continuity conditions for the field and its derivative at the half-period boundary (at $x = c\Lambda$, where the constant c characterizes the filling of the grating — see Fig. 1). The coefficients μ_m in expansions (5) and $\beta_n^{(j)}$ in (4) have the same meaning. The number of real coefficients is limited by the number of radiation diffraction orders, and the coefficient values are related with the effective refractive index of the corresponding mode which is excited by the incident wave in the layer of grating G and in the layers S and M.

Once the expansions of the field in all spatial regions are obtained, the system of linear equations for the unknown mode amplitudes $a_m^{(j)}$ and $b_m^{(j)}$ and amplitudes of diffraction harmonics r_n and t_n is constructed using the continuity conditions at the layer boundaries of the combined grating. Solving this system, we can determine the diffraction efficiency of the grating (R_n and T_n in different orders) as well as the intensity and phase of radiation in any point of space.

3. Interaction of Radiation with the Multilayer Mirror

The interaction of radiation with the multilayer mirror is much simpler than with the diffraction grating and we consider it in more detail. Using the Helmholtz equation (1), we construct the expressions for the

field in all spatial regions:

$$\begin{cases} F_{N+1}(x,y) = \left[r\exp(i\beta_{N+1}y) + r^{(i)}\exp(-i\beta_{N+1}y)\right]e(x), \\ \qquad\vdots \\ F_i(x,y) = [a_i\exp(i\beta_i y) + b_i\exp(-i\beta_i y)]e(x), \\ \qquad\vdots \\ F_0(x,y) = t\exp(-i\beta_0 y)e(x). \end{cases} \tag{6}$$

Here, $e(x) = \exp(i\alpha x)$, $\alpha = kn_{N+1}\sin\theta$, and $\beta_i^2 = k^2n_i^2 - \alpha^2$; $r^{(i)}$, r, and t are the amplitudes of incident, reflected, and transmitted waves, respectively; the subscripts "0" and "$N+1$" denote the lower and higher half-space, respectively. In order to find the unknown amplitudes r and t, we invoke the continuity conditions at the layer boundaries:

$$\begin{aligned} F_i(x,\Sigma_i) &= F_{i+1}(x,\Sigma_i), \\ \sigma_i F'_{yi}(x,\Sigma_i) &= \sigma_{i+1}F'_{yi+1}(x,\Sigma_i), \end{aligned} \tag{7}$$

where $\sigma_i = 1/\mu_i$ for TE polarization and $\sigma_i = 1/\varepsilon_i$ for TH polarization and the designation $\Sigma_i = \sum_{j=0}^{j=i} h_j$ is introduced. Here, μ_i and ε_i are equal to the magnetic permeability and permittivity, respectively, in the ith spatial region. On substituting (2) in (3) and changing the variables, we arrive at the system of linear equations

$$\begin{cases} t = \tilde{a}_1 D_1^- + \tilde{b}_1 D_1^+, \\ -\xi_0 t = \tilde{a}_1 D_1^- - \tilde{b}_1 D_1^+, \\ \qquad\vdots \\ \tilde{a}_i D_i^+ + \tilde{b}_i D_i^- = \tilde{a}_{i+1} D_{i+1}^- + \tilde{b}_{i+1} D_{i+1}^+, \\ \xi_i(\tilde{a}_i D_i^+ - \tilde{b}_i D_i^-) = \tilde{a}_{i+1} D_{i+1}^- - \tilde{b}_{i+1} D_{i+1}^+, \\ \qquad\vdots \\ \tilde{a}_N D_N^+ + \tilde{b}_N D_N^- = \tilde{r} + \tilde{r}^{(i)}, \\ \xi_N(\tilde{a}_N D_N^+ - \tilde{b}_N D_N^-) = \tilde{r} - \tilde{r}^{(i)}. \end{cases} \tag{8}$$

The following designations are introduced here:

$$\begin{aligned} \tau_i^{\pm} &= \exp(\pm i\beta_i h_i/2), \\ e_i &= \exp(i\beta_i h_i), \\ D_i^{\pm} &= \tau_i^{\pm}/(\tau_i^+ + \tau_i^-), \\ \xi_i &= (\sigma_i\beta_i)/(\sigma_{i+1}\beta_{i+1}), \\ \chi_i &= (1-\xi_i)/(1+\xi_i), \\ \tilde{a}_i &= a_i\exp(i\beta_i\Sigma_{i-1})(\tau_i^+ + \tau_i^-)\tau_i^+, \\ \tilde{b}_i &= b_i\exp(-i\beta_i\Sigma_{i-1})(\tau_i^+ + \tau_i^-)\tau_i^-, \\ \tilde{r} &= r\exp(i\beta_{N+1}\Sigma_N), \\ \tilde{r}^{(i)} &= r^{(i)}\exp(-i\beta_{N+1}\Sigma_N), \end{aligned} \tag{9}$$

and it is assumed that $\Sigma_0 = 0$. From Eqs. (8) the recursions follow, which allow one to express all unknown amplitudes in terms of the incident-wave amplitude:

$$\begin{aligned} \tilde{r} &= \frac{\omega_N D_N^+ + D_N^- \chi_N}{\omega_N D_N^+ \chi_N + D_N^-} \tilde{r}^{(i)}, \\ \tilde{b}_N &= \frac{2\tilde{r}^{(i)}}{(1+\xi_N)(\omega_N D_N^+ \chi_N + D_N^-)}, \\ \tilde{b}_{i-1} &= \frac{\omega_i D_i^- + D_i^+}{\omega_{i-1} D_{i-1}^+ + D_{i-1}^-} \tilde{b}_i, \\ t &= (\omega_1 D_1^- + D_1^+)\tilde{b}_1, \end{aligned} \tag{10}$$

where

$$\tilde{a}_i = \omega_i \tilde{b}_i, \qquad \omega_1 = e_1 \chi_0, \qquad \omega_{i+1} = e_{i+1} \frac{\omega_i D_i^+ + D_i^- \chi_i}{\omega_i D_i^+ \chi_i + D_i^-}. \tag{11}$$

Thus, the problem is solved. Using expressions (9)–(11), one can determine the field amplitude in all spatial regions and, thus, the reflectance R and transmittance T of the mirror.

4. Properties of the Simplest Combined Diffraction Grating Set in the Scheme of Grazing Incidence

We begin the study of the combined gratings with the case of the simplest structure, which consists of only two layers. One of them is the layer of the grating G with a rectangular ruling profile and the other is the continuous dielectric layer S. Let the refractive indices of the grating material $n^{(G)}$ and continuous layer $n^{(S)}$ be equal to 1.5, while those of the upper and lower half-spaces are set equal to unity. We set the ratio between the radiation wavelength and the grating period equal to 3/2; in this case, the energy is carried away from the grating only through the specular reflection and a single diffraction order [harmonics with the numbers 0 and -1 in Rayleigh expansions (3)].

Let us investigate the dependence of the diffraction efficiency of the simplest combined grating set in the scheme of grazing incidence (the angle of incidence of radiation on the grating is $\theta = 89°$) on the parameters $h^{(G)}$ and $h^{(S)}$. The chart of the surface layers $R_{-1}(h^{(S)}, h^{(G)})$ is shown in Fig. 2 by the gradations of gray color. As can be seen from the figure, this dependence takes the form of narrow ridges arranged periodically in the plane $(h^{(S)}, h^{(G)})$.

We use mode expansion (5) to analyze the dependence of the diffraction efficiency on the grating depth. The transverse field distribution within the grating is defined by the factors $\exp(\pm i\mu_m y)$. As already noted in Sec. 2, there are several real coefficients in the set μ_m. We have two such coefficients, μ_0 and μ_{-1}, in our case, which can be related to the zeroth and minus first diffraction orders. Since the field distributions periodical in the grating depth correspond to these modes, the former must make a major contribution to the dependence $R_{-1}(h^{(G)})$. To verify this, we enter the condition

$$\begin{cases} \mu_m h^{(G)} = \pi/2 + \pi k, \\ k = 0, 1, \ldots, \end{cases} \tag{12}$$

which defines the thickness of the quarter-wave layer for the mth grating mode. The horizontal lines in Fig. 2 were passed in accordance with condition (12) for the zeroth grating mode (coefficient μ_0). It is readily seen

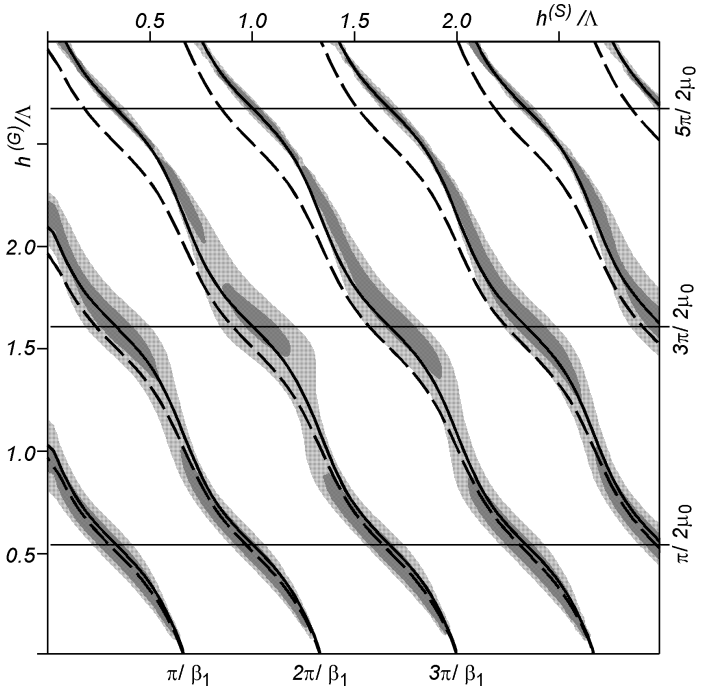

Fig. 2. Dependence of the diffraction efficiency of a two-layer combined grating R_{-1} on the depth of the grating layer $h^{(G)}$ and the thickness of the S layer $h^{(S)}$ (see the text).

that these straight lines pass through the maxima of the $R_{-1}(h^{(S)}, h^{(G)})$ dependence. Thus, the character of the $R_{-1}(h^{(G)})$ dependence is defined primarily by the zeroth grating mode, since its excitation by the incident wave is most efficient at grazing incidence and requirement (12) provides the resonant conditions of excitation. Note, however, that the effect of other grating modes can also be appreciable. For example, for $h^{(G)}$ values, which provide the fulfillment of condition (12) for two modes simultaneously, the efficiency maxima become sharper (see top part of Fig. 2).

We consider now the dependence of the diffraction efficiency on the relationship between the grating depth $h^{(G)}$ and layer thickness $h^{(S)}$. For this purpose, we approximate the grating by the continuous dielectric layer and analyze the interaction of the resulting two-layer mirror $\tilde{\text{G}}$S with the incident radiation. We use the coefficient μ_0 for the calculation of the averaged refractive index $\tilde{n}^{(G)}$ of the layer, which approximates the grating, since the zeroth grating mode was shown to have the main effect on the diffraction efficiency. For this purpose, we use the relationship

$$\mu_0 = k\tilde{n}^{(G)} \cos\tilde{\theta} = k\sqrt{\tilde{n}^{(G)2} - \sin^2\theta}, \tag{13}$$

where θ is the angle of incidence of radiation on the grating and $\tilde{\theta}$ is the "angle of refraction" of the incident wave in the approximating layer. Figure 3 shows the dependence of the refractive index of the approximating layer $\tilde{n}^{(G)}$ on the filling factor of the grating c calculated for various angles of incidence θ on the grating. The dependence $\tilde{n}^{(G)} = cn^{(G)} + (1 - c)$ obtained by the arithmetical averaging of $n^{(G)}$ over the grating period is shown on the same graph by a dashed line. It is readily seen that the refractive index $\tilde{n}^{(G)}$ differs only slightly from this empirical assessment at large angles of incidence.

The condition of the grazing incidence of radiation allows the $\tilde{\text{G}}$S structure to be considered as a two-layer Lummer–Gehrke interferometer or, in modern terms, as a two-layer dielectric waveguide with a small leakage. The interaction of radiation with such structures is known to have a resonant behavior. The

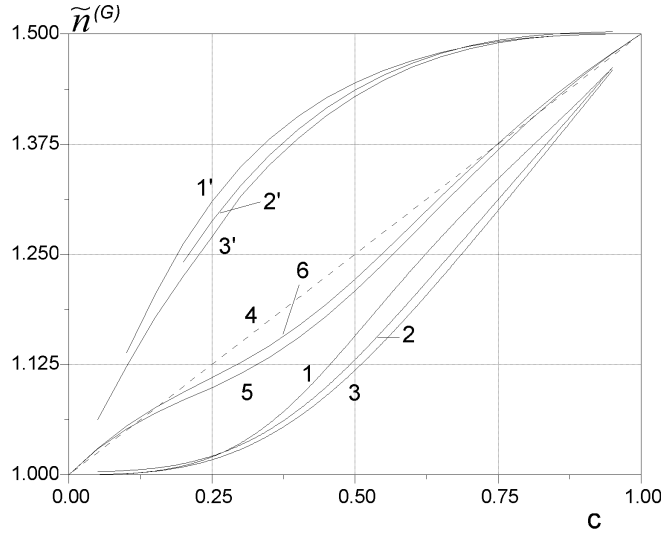

Fig. 3. Dependence of the averaged refractive index $\tilde{n}^{(G)}$ of the layer approximating the grating on the filling factor of the grating c. The angle of incidence θ is equal to 30° (curves 1 and 1′), 49° (curves 2 and 2′), 87° (curves 3 and 3′), 70° (curve 5), and 89° (curve 6). Curves 1, 1′, 2, 2′, 3, and 3′ correspond to the autocollimation mode, and curve 4 is the arithmetical mean of the refractive index over the grating period.

maximum transmission of an interferometer or the excitation of the waveguide mode in it correspond to the occurrence of resonance. We use the results obtained in Sec. 2 to write down the resonance condition. Using formulas (9), (10), and (11), we find the relationship between the amplitudes of the incident and transmitted waves:

$$t = \frac{2r^{(i)}}{c_1c_2\left(1+\frac{\beta_0}{\beta_3}\right) - s_1s_2\left(\frac{\beta_1}{\beta_2}+\frac{\beta_0}{\beta_3}\frac{\beta_2}{\beta_1}\right) - i\left[s_1c_2\left(\frac{\beta_0}{\beta_1}+\frac{\beta_1}{\beta_3}\right)+c_1s_2\left(\frac{\beta_0}{\beta_2}+\frac{\beta_2}{\beta_3}\right)\right]}, \tag{14}$$

where

$$\begin{aligned} c_1 &= \cos(\beta_1 h^{(S)}), & s_1 &= \sin(\beta_1 h^{(S)}, \\ c_2 &= \cos(\beta_2 h^{(G)}), & s_2 &= \sin(\beta_2 h^{(G)}), \\ \beta_1 &= k\sqrt{n^{(S)2} - \sin^2\theta}, & \beta_0 &= k\cos\theta, \\ \beta_2 &= k\sqrt{\tilde{n}^{(G)2} - \sin^2\theta}, & \beta_3 &= k\cos\theta. \end{aligned} \tag{15}$$

The phases of the incident and transmitted waves are known to coincide in the maxima of transmission of the Lummer–Gehrke interferometer. This means that the imaginary part of the denominator of the fraction in expression (14) is equal to zero. By this means we obtain from Eq. (14) the condition for the transverse resonance in the $\tilde{\text{G}}$S structure:

$$\tan(\beta_1 h^{(S)})\left(\frac{\beta_0}{\beta_1}+\frac{\beta_1}{\beta_3}\right) + \tan(\beta_2 h^{(G)})\left(\frac{\beta_0}{\beta_2}+\frac{\beta_2}{\beta_3}\right) = 0. \tag{16}$$

It should be noted that expression (16) coincides with the dispersion equation for the dielectric two-layer leaky-mode waveguide. This suggests the equivalence of the waveguide approach and the way of describing multilayer structures presented in Sec. 3.

We can now compare the resonant properties of the combined grating GS and the waveguide $\tilde{\text{G}}$S. For this purpose, we encounter in Fig. 2 dispersion curves corresponding to the solutions of Eq. (16). The solid lines represent the dispersion curves of the two-layer waveguide with the refractive index of the grating layer $\tilde{n}^{(G)}$ calculated with expression (13), while the dashed lines stand for the case of $\tilde{n}^{(G)}$ calculated with the empirical formula. One can readily see that the dispersion curves virtually perfectly fit the ridges of the dependence $R_{-1}(h^{(S)}, h^{(G)})$. In this case, we can reasonably restrict ourselves to the empirical assessment for $\tilde{n}^{(G)}$ for the gratings of small depth. Thus, we draw the conclusion that the diffraction efficiency of the two-layer combined grating set in the scheme of grazing incidence will be great if the condition of double resonance is met. What this means is, first, the condition for the excitation of the waveguide mode in the structure approximating the combined grating (16) and, second, the resonance condition in the layer of diffraction grating (12). Note that an increase in the refractive index of the material of the grating causes an increase in the number of real coefficients in the set μ_m, i.e., an increase in the number of transverse modes excited. This complicates the interaction behavior and hampers the use of our approach.

5. Optimization of Parameters of the Combined Grating with the Metal Mirror

The results obtained for the simplest model of the combined grating allow one to proceed to studies of more complex and practically significant structures. The actual diffraction gratings are manufactured on a mechanical base (substrate). A metal or dielectric mirror (see Fig. 1) can be used to reduce the penetration of radiation from the combined grating to the substrate and thereby provide the resonant coupling of radiation with a grating. Let us consider a combined grating with a metal film as a mirror M. Let the grating period be 1000 nm, the radiation wavelength be 1500 nm, the angle of incidence of radiation be 89°, $n^{(G)} = n^{(S)} = 1.5$ (quartz), $n^{(M)} = 1.4 + i15$ (aluminum), and the grating have a rectangular profile with the filling factor $c = 0.5$.

Figure 4 presents the dependence $R_{-1}(h^{(S)}, h^{(G)})$ for the grating with an aluminum mirror. The surface layers $R_{-1}(h^{(S)}, h^{(G)})$ are depicted as the gradations of gray color, while the regions of high absorption of the grating are shown by hatching. We repeat for this grating the search procedure for the best values of $h^{(G)}$ and $h^{(S)}$ described above. We find the refractive index of the top layer of the waveguide, which approximates the grating, with expression (13). Since the refractive index of the waveguide substrate is a complex number, there is no way to separate the real and imaginary parts in expression (14) in an explicit form. Therefore, the dispersion equation for the two-layer waveguide on the metal substrate takes the form

$$\text{Im}\left\{c_1c_2\left(1+\frac{\beta_0}{\beta_3}\right)-s_1s_2\left(\frac{\beta_1}{\beta_2}+\frac{\beta_0}{\beta_3}\frac{\beta_2}{\beta_1}\right)-i\left[s_1c_2\left(\frac{\beta_0}{\beta_1}+\frac{\beta_1}{\beta_3}\right)+c_1s_2\left(\frac{\beta_0}{\beta_2}+\frac{\beta_2}{\beta_3}\right)\right]\right\}. \qquad (17)$$

The solutions of this equation corresponding to excitation of the waveguide modes in the structure $\tilde{\text{G}}$SM are shown in Fig. 4 by the solid curves. The grating-depth values satisfying condition (12) are marked off by horizontal straight lines. One can see from Fig. 4 that the dispersion curves pass through the regions of high diffraction efficiency of the grating. Thus, the waveguide properties of the combined grating are retained when using the metal mirror.

The level of radiation absorption is a no less important criterion than the diffraction efficiency in the determination of the optimum parameters of the metal–dielectric combined grating. As is seen from Fig. 4, the regions of high grating absorption coincide with the resonances in the waveguide $\tilde{\text{G}}$SM. Figure 5 shows the variations of the diffraction efficiency and ratio between the grating absorption and efficiency with the position of the point $(h^{(S)}, h^{(G)})$ in the dispersion curve (curve a–a in Fig. 4). The abscissa is the false coordinate ξ. The unity corresponds to the first resonance; three designates the second one. As is illustrated in Fig. 4, the

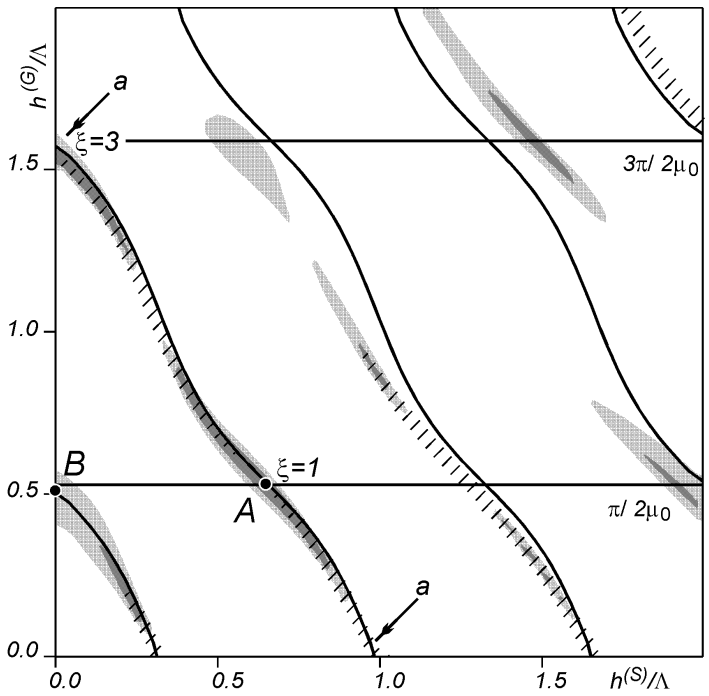

Fig. 4. Dependence of the diffraction efficiency R_{-1} of the metal–dielectric combined grating on the depth of the grating layer $h^{(G)}$ and the thickness of the S layer $h^{(S)}$ (see the text).

grating efficiency is somewhat lower in the points of double resonance ($\xi = 1, 3$), but the absorption–efficiency ratio becomes the best. In the points $\xi = 0, 2$, we have resonance absorption rather than the high efficiency of grating. Thus, the method of optimization proposed may work well for the combined gratings with a metal mirror. The condition for double resonance allows one to determine the grating parameters with high efficiency and optimum efficiency–absorption relationship.

In closing this section, we consider the effect of the grating geometry on the width of the spectral range in which the grating still retains its high efficiency. Figure 6 shows the dependences of the grating efficiency on the radiation wavelength constructed for two lower grating resonances (denoted by the letters A and B in Fig. 4). It is readily seen that for the grating with the minimum interlayer thickness (point B) the diffraction efficiency is rather small, but the spectral range of the grating is wide. For the grating parameters corresponding to the point A, the resonant properties of the grating are more pronounced. This causes an increase in the diffraction efficiency and narrowing of the efficiency maximum on the wavelength scale.

6. Combined Gratings with the Multilayer Dielectric Mirror

The main drawbacks of the combined diffraction gratings with a metal mirror are poor radiation stability and appreciable absorption resulting from the finite conductivity of the metal. In this connection, the studies of combined gratings with a multilayer dielectric mirror are of prime practical significance. The mirror, which consists of alternating quarter-wave layers with high and low refractive index, can be used in the simplest case. The layer width h of such a mirror is known to be defined from the condition

$$h\sqrt{n^2 - \sin^2\psi} = \lambda/4, \tag{18}$$

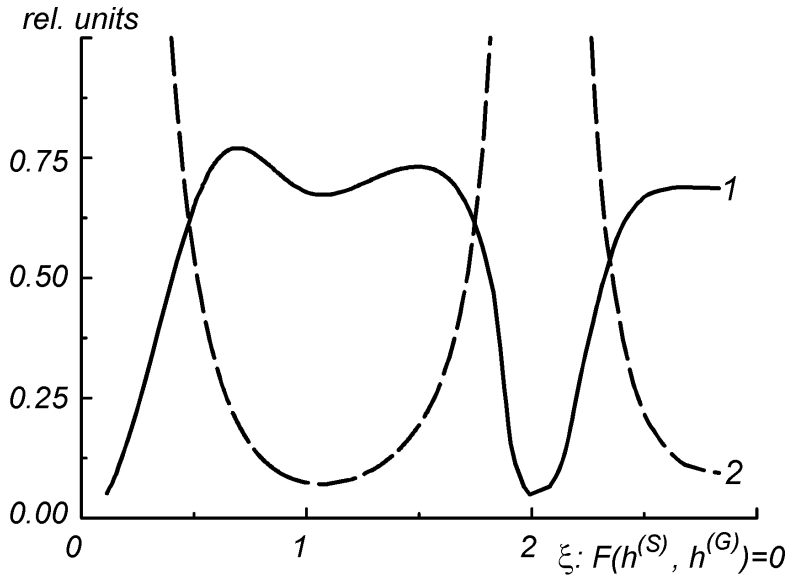

Fig. 5. Dependence of the parameters of the metal–dielectric combined grating on the position of the point $(h^{(S)}, h^{(G)})$ in the dispersion curve (see the text). Curve 1 is the diffraction efficiency; curve 2 is the ratio between the absorption and efficiency.

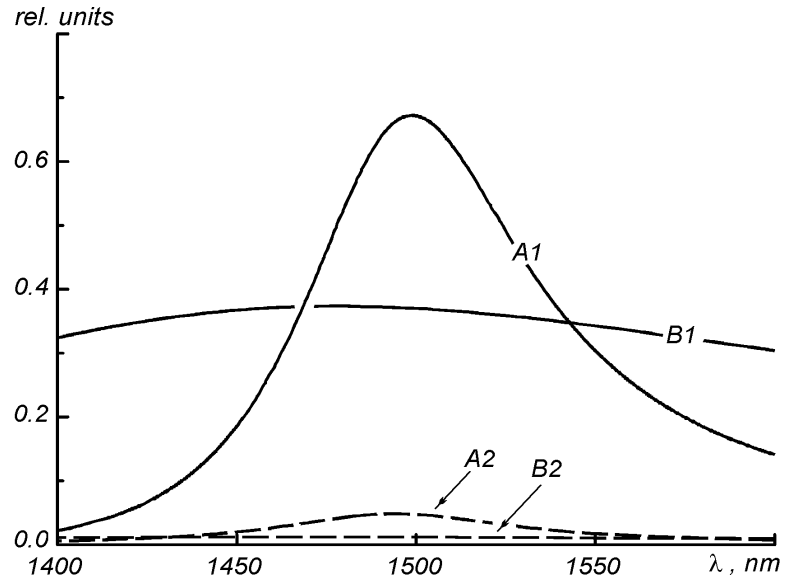

Fig. 6. Dependence of the parameters of the metal–dielectric combined grating on the radiation wavelength λ. Curves A1 and A2 are respectively the diffraction efficiency and absorption at the grating parameters corresponding to the point A in Fig. 4. Curves B1 and B2 are the diffraction efficiency and absorption at the grating parameters corresponding to the point B in Fig. 4.

where λ is the radiation wavelength, n is the refractive index of the layer material, and ψ is the angle of incidence of radiation onto the mirror. Our calculations show that the concrete value of the parameter ψ does not have a profound impact on the properties of the combined grating. Figure 7 shows the dependences of the maximum diffraction efficiency of the combined grating on the number of mirror layers for ψ values equal to the angle of incidence of radiation onto the grating $\theta = 89°$, diffraction angle $\varphi = 30°$, and the

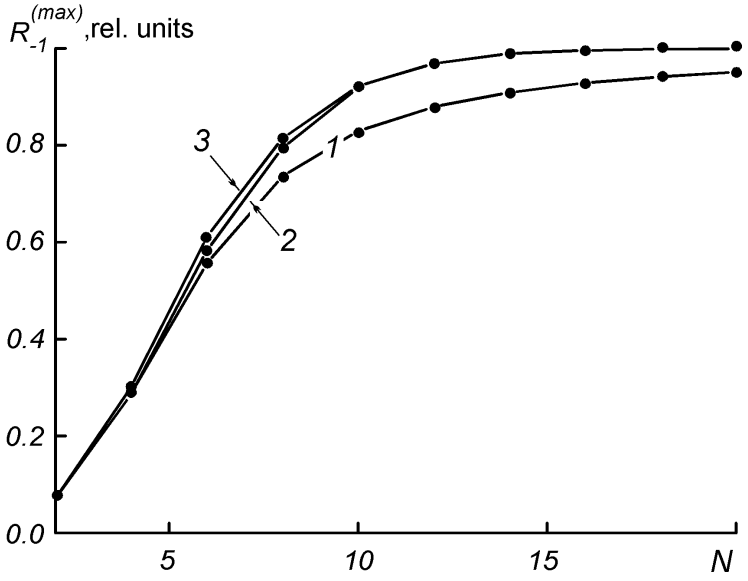

Fig. 7. Dependence of the maximum diffraction efficiency $R_{-1}^{(\max)}$ of the combined grating with the multilayer mirror on the number of mirror layers N. Curve 1 corresponds to $\psi = \theta$; curve 2, $\psi = \varphi$; and curve 3, $\psi = (\theta + \varphi)/2$ (see the text).

arithmetic mean of the incidence and diffraction angles. The maximum diffraction efficiency of the grating was determined through direct numerical optimization. The refractive indices of the grating G and interlayer S were equal to 1.5, the refractive indices of the mirror layers were 1.5 and 2.5, and the rest of the parameters of the problem were the same as in Sec. 5. As is seen from Fig. 7, the efficiency of the combined grating rapidly increases with the number of layers N and reaches virtually the maximum value at $N > 20$. The grating with $\psi = (\theta + \varphi)/2$ possesses the best characteristics because in this case the mirror has the highest reflectivity both for the incident and diffracted radiation.

Figure 8 shows the chart of the surface layers $R_{-1}(h^{(S)}, h^{(G)})$ for the combined grating with the number of mirror layers $N = 20$ and parameter $\psi = (\theta + \varphi)/2$. We approximate the corrugated layer of the combined grating by the continuous dielectric layer and consider the properties of the multilayer mirror obtained. Derivation of the analytical expressions for the radiation transmitted and reflected by the mirror presents difficulties with an increase in the number of layers. Because of this, the mirror parameters were determined analytically with recursions (10) and (11) obtained in Sec. 3. The solid curves in Fig. 8 show the ranges of $h^{(G)}$ and $h^{(S)}$ at which the phases of the waves incident and transmitted through the mirror coincide, i.e., the condition of transverse resonance is met. One can see from Fig. 8 that the coincidence of the waveguide resonances and regions of high diffraction efficiency of the grating occurs also in the case of a large number of dielectric layers.

Figure 9 shows the dependences of the diffraction efficiencies of the combined gratings with various numbers of mirror layers N on the wavelength of radiation. The angle of incidence of radiation on the grating is 89°. In this case, the diffraction efficiency of the combined grating with a multilayer mirror is as much as 100%, being several times higher than that of a conventional grating with a metal coating (the corresponding dependence for such a grating is shown by the dashed line). The width of the peaks of diffraction efficiency of the combined grating is lower than in the case of the metal–dielectric combined grating (see Fig. 6). It is conceivable that one can overcome this disadvantage of the purely dielectric grating by a more sophisticated choice of the multilayer-mirror parameters.

In the analysis of the properties of combined gratings, we restricted our consideration to the case of the

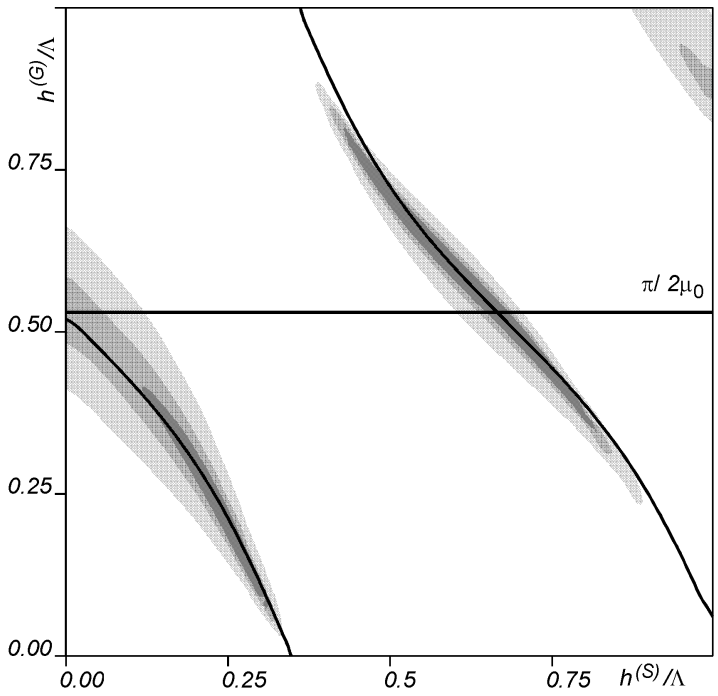

Fig. 8. Dependence of the diffraction efficiency R_{-1} of the combined grating with the multilayer mirror on the parameters $h^{(G)}$ and $h^{(S)}$ (see the text).

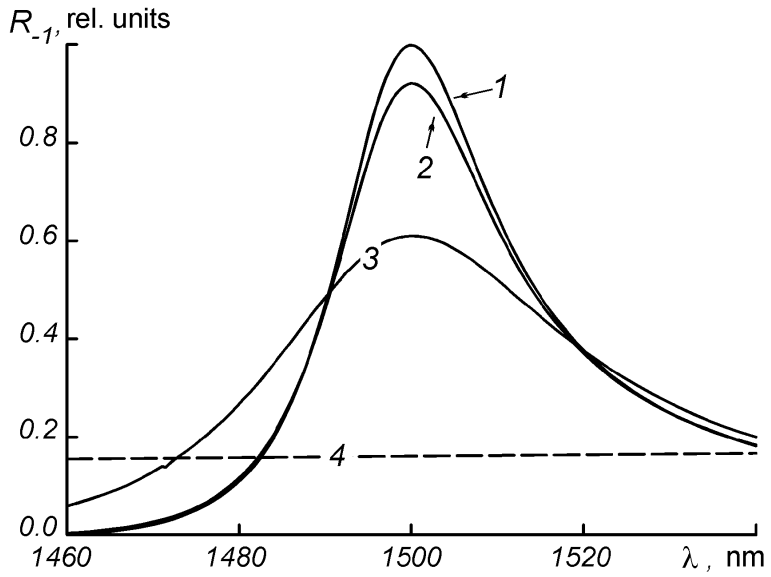

Fig. 9. Dependence of the diffraction efficiency R_{-1} of the combined grating with the multilayer mirror on the radiation wavelength λ. Curve 1 corresponds to $N = 20$; curve 2, $N = 10$; curve 3, $N = 6$; and curve 4 is the dependence for the aluminum grating of the sinusoidal profile.

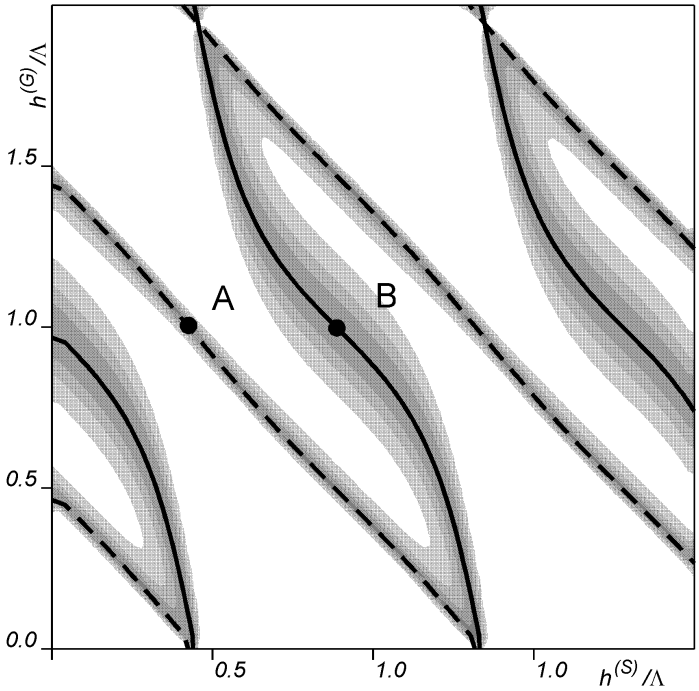

Fig. 10. Dependence of the diffraction efficiency R_{-1} of the combined grating with the multilayer mirror on the parameters $h^{(G)}$ and $h^{(S)}$ when the grating is set to the autocollimation mode (see the text).

grazing incidence. From the standpoint of the waveguide approach, such illumination geometry implies a small leakage in the waveguide. Thus, the resonant behavior of interaction of the incident radiation with the grating and its waveguide properties are quite pronounced. However, our approach proves to be well suited for the study of the combined gratings at any angle φ, including $\varphi = \psi$, i.e., under the condition of waveguide propagation of radiation diffracted by the grating. The chart of the surface layers $R_{-1}(h^{(S)}, h^{(G)})$ for the dielectric combined grating set in the autocollimation mode is shown in Fig. 10. This chart was obtained at $n = 20$, $\psi = \theta \approx 87°$. The wavelength was adjusted to obtain the autocollimation mode; the rest of the grating parameters were the same as in the calculation of Fig. 8. The solid curves show the regions of excitation of the waveguide modes of a multilayer waveguide with refractive index $\tilde{n}^{(G)}$ of the layer approximating the grating, which corresponds to the coefficient μ_0 in expansion (5), while the dashed curves correspond to the coefficient μ_{-1}. It was inferred from Fig. 10 that the waveguide behavior of the interaction of radiation with the grating substantially enriches the surface-layer pattern $R_{-1}(h^{(DS)}, h^{(G)})$ in the case of autocollimation reflection of light. New ranges of the grating parameters at which high diffraction efficiency of the grating is achieved arise in this pattern. The localization of these ranges in the vicinity of the dispersion curves of the layer structure, in which the refractive index $\tilde{n}^{(G)}$ of the layer approximating the grating is defined by the coefficient μ_{-1}, generates a need for deeper insight into their origin. Note, first of all, that the condition of the autocollimation reflection of light corresponds to that of resonant coupling of the leaky modes in the corrugated waveguide:

$$\Lambda = \frac{\lambda}{2\sin\theta} \qquad \text{and} \qquad n^* = \sin\theta \longrightarrow \Lambda = \frac{\lambda}{2n^*} \,. \tag{19}$$

This means that upon the autocollimation reflection two counterpropagating waves are excited in the corrugated waveguide. These waves interfere, producing various distributions of the optical field at the grating. The localization of this distribution relative to the grating depends on the phase of the reflected

wave. The calculation of this phase in the points A and B belonging to the dispersion curves in Fig. 10 showed that the phase difference for the reflected and incident waves was equal to π. The distribution of the field amplitude $u_m(x)$ relative to the grating in the points A and B was also calculated. In the point A the field was shown to be mainly localized in the grooves of the diffraction grating, while in the point B, outside of them. In our judgment, such a difference of the field distributions in the grating is the physical cause of the appearance of two values of the refractive index $\tilde{n}^{(G)}$ of the layer, which approximates the dielectric grating. Variations in $\tilde{n}^{(G)}$ with the filling factor of the grating for various autocollimation angles are presented in Fig. 3. It is apparent that the use of the single value of $\tilde{n}^{(G)}$ in the case of autocollimation reflection, which is defined by the expression

$$\tilde{n}^{(G)} = cn^{(G)} + (1 - c), \tag{20}$$

gives the averaged pattern of the levels of the function $R_{-1}(h^{(S)}, h^{(G)})$. This pattern will be close to the actual one at small grating depths ($h^{(G)} < 0.3\Lambda$), which are of practical significance.

7. Conclusions

In this paper, the results of investigation of the properties of combined diffraction gratings were presented, based on the modal approach to the solution of the diffraction problem. The high diffraction efficiency of grating when operating in the scheme of grazing incidence was shown to be due to the occurrence of transverse resonances in the combined structure. In this case, the resonant properties of the combined grating were found to be equivalent to the properties of the dielectric waveguide. The coincidence of properties of the grating and the waveguide approximating it allows one to determine the optimum parameters of the combined grating by the solution of the dispersion equations for the layer structures rather than from the solution of the diffraction problem. This greatly simplifies the optimization procedure.

The waveguide behavior of the interaction of radiation with the combined grating was shown to be manifested not only when it was set in the scheme of grazing incidence, but also in other operation modes, e.g., in the autocollimation mode.

The use of the analogy between the properties of the grating and the waveguide exhibits the most promise for these studies and for optimization of the gratings combined with a multilayer dielectric mirror since the direct numerical optimization of such structures presents difficulties.

Acknowledgments

The authors are grateful to S. K. Borisov for helpful discussions. This work was supported by the Russian Foundation for Basic Research (Grant No. 00-02-17442).

References

1. A. S. Svakhin, V. A. Sychugov, and A. E. Tikhomirov, *Zh. Tekh. Fiz.*, **61**, 124 (1991).
2. M. D. Perry, R. D. Boud, J. A. Britten, et al., *Opt. Lett.*, **20**, 940 (1995).
3. B. W. Shore, M. D. Perry, J. A. Britten, et al., *J. Opt. Soc. Am. A*, **14**, 1124 (1997).
4. I. F. Salakhutdinov, V. A. Sychugov, and O. Par'e, *Kvantovaya Élektron.*, **25**, 1009 (1998).
5. S. V. Vasil'ev, *Kvantovaya Élektron.*, **25**, 429 (1998).
6. I. C. Botten, M. S. Craig, R. C. McPhedran, et al., *Optica Acta*, **28**, 413 (1981).